Journal of Chemistry and Technologies, 2026, *34*(1), 71-85

Journal of Chemistry and Technologies

pISSN 2663-2934 (Print), ISSN 2663-2942 (Online).

journal homepage: http://chemistry.dnu.dp.ua
editorial e-mail: chem.dnu@gmail.com

UDC 620.3:544.72:628.16

SYNTHESIS AND CHARACTERIZATION OF ZrO_2@Fe_3O_4@TSC MAGNETIC NANOCOMPOSITE FOR SUSTAINABLE REMEDIATION OF HEAVY METAL FROM CONTAMINATED WATER

Govinda Varadhi[1*] R. Sarada[2], K.V. Padmavathi[1], R. Kishore[3], A. Karteek Rao[1], Ch.V. Kameswara Rao[4]

[1]*Department of Chemistry, Gayatri Vidya Parishad College for Degree and PG Courses (A), Visakhapatnam-530045, Andhra Pradesh, India.*

[2]*Department of Chemistry, Anil Neerukonda Institute of Technology and Science, Visakhapatnam-531162, Andhra Pradesh, India.*

[3]*Department of Chemistry, Gitam to be University, Visakhapatnam-530045, Andhra Pradesh, India.*

[4]*Department of Chemistry, Lendi Institute of Engineering and Technology, Vizianagaram-535005, Andhra Pradesh, India.*

Received 25 October 2025; accepted 3 February 2026; available online 23 March 2026

Abstract

This study presents the synthesis and characterization of a novel adsorbent composed of iron oxide and zirconium oxide magnetic nanoparticles (ZrO_2@Fe_3O_4 MNPs) functionalized with trisodium citrate (TSC). The structural and physicochemical properties of the ZrO_2@Fe_3O_4@TSC nanocomposite were systematically investigated using Fourier-transform infrared spectroscopy (FTIR), X-ray diffraction (XRD), transmission electron microscopy (TEM) and vibrating sample magnetometry (VSM). The characterization results established that the ZrO_2@Fe_3O_4@TSC nanocomposite shows a spherical morphology with particle sizes ranging from 16 to 20 nm. Magnetic measurements indicated that the nanocomposite possesses ferromagnetic behavior with a saturation magnetization value of 7.71 emu/g. The adsorption narration of the ZrO_2@Fe_3O_4@TSC nanocomposite was evaluated for the removal of Cd (II) ions from aqueous solutions. The adsorption kinetics closely followed the pseudo-second-order model, demonstrating chemisorption as the leading process. The adsorption isotherm data were well described by the Langmuir isotherm model, suggesting monolayer adsorption on a homogenous surface. The maximum adsorption capacity was determined to be 50.26 mg/g at 303 K. These findings highlight the potential of ZrO_2@Fe_3O_4@TSC nanocomposites as efficient adsorbents for heavy metal remediation in wastewater treatment applications.

Keywords: wastewater treatment; ZrO_2@Fe_3O_4@TSC nanocomposite; TEM; VSM; XRD and FTIR.

СИНТЕЗ ТА ХАРАКТЕРИСТИКА МАГНІТНОГО НАНОКОМПОЗИТУ ZRO_2@FE_3O_4@TSC ДЛЯ ЕКОЛОГІЧНО БЕЗПЕЧНОГО ВИДАЛЕННЯ ВАЖКИХ МЕТАЛІВ ІЗ ЗАБРУДНЕНОЇ ВОДИ

Говінда Варадхі[1*], Р. Сарада[2], К.В. Падмаваті[1], Р. Кішоре[3], А. Картік Рао[1], Ч.В. Камешвара Рао[4]

[1]*Кафедра хімії, Коледж Гаятрі Відя Парішад для отримання ступеня та післядипломної освіти (А), Вішакхапатнам-530045, Андхра-Прадеш, Індія.*

[2]*Кафедра хімії, Інститут технології та науки імені Аніла Неруконди, Вішакхапатнам-531162, Андхра-Прадеш, Індія.*

[3]*Кафедра хімії, Університет Гітам-ту-бі, Вішакхапатнам-530045, Андхра-Прадеш, Індія.*

[4]*Кафедра хімії, Інститут інженерії та технології імені Ленді, Візіанагарам-535005, Андхра-Прадеш, Індія.*

Анотація

У цьому дослідженні представлено синтез та характеристику нового адсорбенту, що складається з магнітних наночастинок оксиду заліза та оксиду цирконію (ZrO_2@Fe_3O_4 MNPs), функціоналізованих тринатрійцитратом (TSC). Структурні та фізико-хімічні властивості нанокомпозиту ZrO_2@Fe_3O_4@TSC були систематично досліджені за допомогою інфрачервоної спектроскопії з Фур'є-перетворенням (FTIR), рентгенівської дифракції (XRD), просвічувальної електронної мікроскопії (TEM) та магнітометрії з вібраційною пробою (VSM). Результати характеристик встановили, що нанокомпозит ZrO_2@Fe_3O_4@TSC має сферичну морфологію з розмірами частинок від 16 до 20 нм. Магнітні вимірювання показали, що нанокомпозит має феромагнітні властивості з величиною насиченої намагніченості 7.71 emu/г. Адсорбційні властивості нанокомпозиту ZrO_2@Fe_3O_4@TSC оцінювали для видалення іонів Cd (II) з водних розчинів. Кінетика адсорбції тісно відповідала моделі псевдодругого порядку, що свідчить про хімічну адсорбцію як провідний процес. Дані адсорбційної ізотерми добре описувалися моделлю ізотерми Ленгмюра, що вказує на одношарову адсорбцію на однорідній поверхні. Максимальна адсорбційна здатність була визначена на рівні 50 /26 мг/г за 303 К. Ці результати підкреслюють потенціал нанокомпозитів ZrO_2@Fe_3O_4@TSC як ефективних адсорбентів для видалення важких металів у системах очищення стічних вод.

Ключові слова: очищення стічних вод; нанокомпозит ZrO_2@Fe_3O_4@TSC; TEM; VSM; XRD та FTIR.

**Corresponding author: e-mail: varadhigovinda47@gmail.com*

Introduction

Over the past few decades, the development of alloyed nanocomposites – including those based on TiO_2, ZnO, Fe_2O_3, and CuO – has become increasingly important and has attracted significant attention in the context of environmentally friendly treatment of industrial wastewater contaminated with heavy metals. The combination of metallic dopants such as Zr, Au, Cu, Pt, Fe and Ag enhances the adsorption abilities and catalytic activity of these materials, facilitating the removal of pollutants from wastewater through adsorption and active site interactions [1–4]. However, the scientific society is also mainly concerned with addressing the ongoing environmental crisis and mitigating the antagonistic effects of various harmful pollutants which are released by industrial facilities. [5–7]. Hence, researchers are actively exploring sustainable solutions to minimize environmental degradation and promote eco-friendly components. Among these materials, therefore, Fe-doped ZrO_2 nanoparticles ($Fe@ZrO_2$) have shown significant potential in the field of wastewater applications [8–11]. Previous reports have also indicated that Fe incorporation into metal oxides can improve the adsorption efficiency by modifying the surface properties and electronic structure of the nanocomposite [12–15].

Furthermore, Fe-doped ZrO_2 and CuS display promising photocatalytic properties, making them effective catalysts for the degradation of Rhodamine B dye under visible-light irradiation. The synergistic effect of Fe and Zr enhances charge separation, minimizes electron-hole recombination and encompasses the absorption range into the visible spectrum, thus improving overall photocatalytic performance [16; 17]. Additionally, recent research has highlighted the potential of dolomite-quartz@Fe_3O_4 nanocomposites as highly efficient adsorbents for heavy metal remediation, particularly in the removal of cadmium (Cd^{2+}) from contaminated water sources [5; 18]. This approach is vital for extenuating the pollution of aquatic ecosystems including lakes, rivers and soil environments, which are caused by heavy metal discharge from industrial activities. Further, the reports highlight promising applications for $ZrO_2@Fe_3O_4$ MNPs) nanoparticles functionalized with trisodium citrate (TSC). Moreover, this present study aims to explore its adsorption capability for heavy metal removal. The results of this study may also contribute to the development of wastewater treatment strategies using nanomaterials, which, in turn, opens up opportunities for creating environmentally friendly solutions in the field of environmental pollution control. This study examines the synthesis, characterization, and application of $ZrO_2@Fe_3O_4$@TSC nanocomposites for the removal of Cd(II) from wastewater. Furthermore, it can be concluded that the adsorption of impurities from industrial wastewater, which follows a pseudo-second-order kinetic model and the Langmuir isotherm, is capable of describing the adsorption process on the $ZrO_2@Fe_3O_4$@TSC nanocomposite.

However, the rapid enhancement of urbanization and industrialization over the past few decades have significantly contributed to ecological pollution, leading to harmful effects on ecosystems and human health [19-21]. Consequently, the rapid expansion of urban areas and the growth of industrial activity have led to increased emissions of pollutants into the air, water, and soil, exacerbating environmental imbalances and posing a serious threat to public health [22–24]. The contamination of water bodies with heavy metals represents a critical public health problem due to their unembellished toxicological impacts on both ecosystems and human health. Among several reports, cadmium (Cd^{2+}), mercury (Hg^{2+}) and lead (Pb^{2+}) are classified as highly hazardous heavy metal ions, which raises significant environmental concerns. In particular, Cd^{2+} ion is one of the tremendously toxic heavy metal ions often detected in industrial wastes. It is primarily released as a result of certain activities, such as pigment production, electroplating, mining, metallurgical processes, and plastics manufacturing, and poses a significant threat to aquatic flora and fauna, as well as to the general public [25–27]. Cadmium (Cd (II)) is an extremely poisonous heavy metal with not at all acknowledged the biological function in the human body and its exposure has been related to unembellished health problems, including emphysema [28; 29] diabetes mellitus [30; 31], renal dysfunction [32; 33], osteoporosis [34; 35] and skeletal distortions [36; 37] due to its ability to dislocate owed to the lack of homeostatic control for Cd (II) in the human body. The non-biodegradable nature of Cd (II) and its strong bioaccumulative properties require the development of efficient and steadfast remediation strategies for its removal from contaminated water sources.

Numerous physicochemical and biological methods have been investigated for the detection

and removal of heavy metals such as Cd(II), Pb(II), and As(III), including electrochemical methods, chemical precipitation, membrane filtration, colorimetric detection, flotation, coagulation, biosorption, and microbial remediation. Among these approaches, adsorption has received considerable attention because of its high efficiency, low cost, and environmental compatibility. Recent advances in nanotechnology and functionalized adsorbents, including biochar, metal-organic frameworks, and graphene-based composites, have further improved the selectivity and adsorption capacity of materials used for Cd(II) removal from water. These developments highlight the need for continued research aimed at optimizing Cd(II) removal technologies and addressing the environmental and health risks associated with heavy metal contamination.

The present study is aimed at developing a cost-effective and high-performance nanocomposite for the removal of Cd(II) from industrial wastewater. Owing to their large specific surface area and the possibility of surface functionalization, nanocomposites provide a high density of active sites and therefore enable efficient adsorption of cadmium ions. However, practical limitations associated with conventional nanomaterial-based adsorption systems have restricted their wider application. Among various nanomaterials, magnetic nanocomposites have been extensively used in water treatment, catalysis, and biomedical applications because of their unique magnetic properties. In wastewater treatment, they are particularly attractive as adsorbents for heavy metal removal because they can be rapidly separated from aqueous media using an external magnetic field. Fe_3O_4-based magnetic nanocomposites are especially promising for the remediation of heavy-metal-contaminated industrial effluents due to their high adsorption capacity, thermal stability, cost-effectiveness, and facile recovery and reuse. On this basis, the present work proposes an economical and efficient magnetic nanocomposite for Cd(II) removal from wastewater.

Materials and Methods

Synthesis of ZrO_2/Fe_3O_4 magnetic nanoparticles

Fe_3O_4 nanoparticles were synthesized by the co-precipitation method, in which Fe^{2+} and Fe^{3+} ions were reacted with ammonium hydroxide under controlled conditions. A 0.1 g portion of the prepared Fe_3O_4 nanoparticles was dispersed in a binary solvent mixture containing 20 % ethanol and 80 % distilled water to obtain a homogeneous suspension. Subsequently, 1 mL of ammonia solution was added dropwise under continuous stirring for 1 h to promote nucleation and stabilization of the nanoparticles. An aqueous solution of zirconium oxychloride ($ZrOCl_2$) was then introduced, followed by the addition of 30 % NH_3 solution to facilitate the formation of zirconium-modified Fe_3O_4 nanoparticles. The reaction mixture was stirred for an additional 3 h to enhance the interaction between Fe_3O_4 and the zirconium precursor. The resulting mixture was refluxed under optimized thermal conditions to improve crystallinity and phase purity. Finally, the product was collected by filtration, thoroughly washed to remove unreacted precursors, and sintered at 250 °C for 3 h to obtain the desired nanocomposite.

Synthesis of ZrO_2@Fe_3O_4@TSC magnetic nanocomposites

The synthesized ZrO_2@Fe_3O_4 magnetic nanoparticles were redispersed in 100 mL of a 0.6 M trisodium citrate (TSC) solution and heated at 80 °C under ultrasonication for 60 min. This treatment enabled the functionalization of the nanoparticle surface with TSC and improved the dispersion stability of the magnetic nanocomposite. The obtained ZrO_2@Fe_3O_4@TSC product was then separated, washed, and dried for further characterization and adsorption studies.

Batch adsorption experiments

This experimental study suggests that while adsorption is an effective accomplishment method and further fashionable method than other methods due to the material consisting of physicochemical properties and preparation techniques. However, adsorption method is useful to reduce costs effectiveness, naturally occurring adsorbents such as clay minerals, soil-based materials and other low-cost alternatives are widely utilized. In batch adsorption experiments, nonetheless, a fixed amount of adsorbent is introduced into a solution containing the target adsorbate at a known concentration. It is easier method to know and understand the adsorption mechanisms and surface interactions of adsorbate and adsorbent. Moreover, the effect of key parameters such as pH, temperature, contact time and adsorbent dosage is analyzed to optimize adsorption implementation. Indeed, the chemical analyzing sample is when disturbed under controlled conditions such as temperature, concentration and pH, then it allows to reach equilibrium. The amount adsorbed per unit mass of adsorbent is to be determined using the mass

Journal of Chemistry and Technologies, 2026, *34*(1), 71-85

balance equation, after the remaining adsorbate concentration in the sample is measured.

The adsorption behavior of Cd (II) ions onto ZrO_2@Fe_3O_4@TSC nanocomposites was scientifically examined through batch adsorption experiments in an aqueous medium. The pH of the solution was varied from 2 to 8, and the experimental sample solutions were conducted at a constant temperature of 303 K. The Cd (II) stock solution was prepared with different concentrations and 4.5 mg of the magnetic nano-adsorbent was introduced into 25 mL of each Cd (II) ion solution. The primary pH of the solution was exactly adjusted using 0.1 M HCl or NaOH solution. Individually each sample mixture was subjected to ultrasonication at room temperature for 10 minutes, followed by transfer to a 100 mL Erlenmeyer flask. The sample solution was then disquieted in a thermostatic incubator at 200 rpm and 303 K to smooth adsorption. After this whole process, the magnetic nano adsorbent was separated from the solution by using an external magnetic field. The residual concentration of Cd (II) ions in the solution was determined with aid of Flame Atomic Absorption Spectroscopy (FAAS, Shimadzu AA-6300). All adsorption tests were made in triplicate to confirm reproducibility with precisely. The balance in the adsorption capacity of Cd (II) ions by the ZrO_2@Fe_3O_4@TSC nanocomposites was calculated using the following equations:

Hence, to determine an amount of Cd (II) adsorbed and % of adsorbed in the industrial wastewater by ZrO_2@Fe_3O_4@TSC nanocomposites at equilibrium was obtained using the following equation.

$$q_e = \frac{(C_i - C_e)V}{m} \qquad (1)$$

where qe (mg/g) is the equilibrium adsorption capacity of Cd (II). Ci and Ce were initial and equilibrium concentrations (mg/L) of Cd (II) respectively. m is the adsorbent dosage (mg), V is the volume of the solution (L) and also the adsorption percentage was defined as follows:

$$Adsorption(\%) = \frac{(C_i - C_e)}{C_i} \times 100 \qquad (2)$$

Experimental of Adsorption Kinetics for Cd (II)

The adsorption of Cd(II) was investigated at pH 6.0 as a function of contact time and temperature using ZrO_2@Fe_3O_4@TSC as the adsorbent. The results showed that the adsorption capacity increased with increasing temperature, indicating that the process was endothermic. In addition, the time required to reach adsorption equilibrium decreased from 60 min to 30 min as the temperature increased. The adsorption kinetics were analyzed using the amount adsorbed, q_t (mg/g), as a function of time, t (min). The kinetic data were fitted to the pseudo-second-order model by plotting t/q_t versus t, and an excellent correlation coefficient (R^2 = 0.999) was obtained. These results indicate that the pseudo-second-order model provides an appropriate description of Cd(II) adsorption onto the ZrO_2@Fe_3O_4@TSC nanocomposite.

Characterization techniques

FTIR analysis of the synthesized ZrO_2@Fe_3O_4@TSC magnetic nanoparticles was carried out using a Thermo Nicolet FTIR-200 spectrometer at room temperature. Powder X-ray diffraction patterns were recorded with a Bruker AXS D8 Advance diffractometer using Cu Kα radiation (λ = 0.15406 nm) operated at 40 kV and 30 mA, with a scan rate of 0.02° min^{-1} over a 2θ range of 5° to 80°. The morphology and particle size distribution of the obtained ZrO_2@Fe_3O_4@TSC nanoparticles were examined by transmission electron microscopy using a JEOL JEM-3010 instrument operated at 200 kV. The magnetic properties of the synthesized nanocomposite were measured using a Lake Shore vibrating sample magnetometer (VSM-7410). These characterization techniques were employed to evaluate the structural, morphological, and magnetic properties of the synthesized ZrO_2@Fe_3O_4@TSC nanocomposite.

Results and discussion

FTIR spectrum study

The FTIR spectra of ZrO_2@Fe_3O_4 and ZrO_2@Fe_3O_4@TSC magnetic nanoparticles are shown in Figure 1A. The broad absorption band at 3448 cm^{-1} is attributed to the stretching vibration of O–H groups, indicating the presence of surface hydroxyl groups that may participate in hydrogen-bonding interactions. The characteristic bands at 578 cm^{-1} and 476 cm^{-1} correspond to Fe–O and Zr–O stretching vibrations, respectively, confirming the successful incorporation of Fe_3O_4 and ZrO_2 into the nanocomposite structure. After functionalization with TSC, the FTIR spectrum of ZrO_2@Fe_3O_4@TSC showed noticeable shifts in the metal-oxygen bands, with the Zr–O and Fe–O stretching vibrations appearing at 470 cm^{-1} and 565 cm^{-1}, respectively. These shifts indicate strong interactions between the citrate ligand and the metal oxide framework, likely through coordination bonding. In addition, the bands observed at 1410 cm^{-1} and 1615 cm^{-1} are

Journal of Chemistry and Technologies, 2026, *34*(1), 71-85

assigned to the symmetric and asymmetric stretching vibrations of carboxylate groups, confirming the successful conjugation of TSC on the nanoparticle surface. The bands at 2935 cm^{-1} and 2870 cm^{-1} are attributed to C–H stretching vibrations, further supporting the presence of organic functional groups. Overall, the FTIR results confirm the effective functionalization of ZrO_2@Fe_3O_4 nanoparticles with TSC.*XRD pattern analysis*

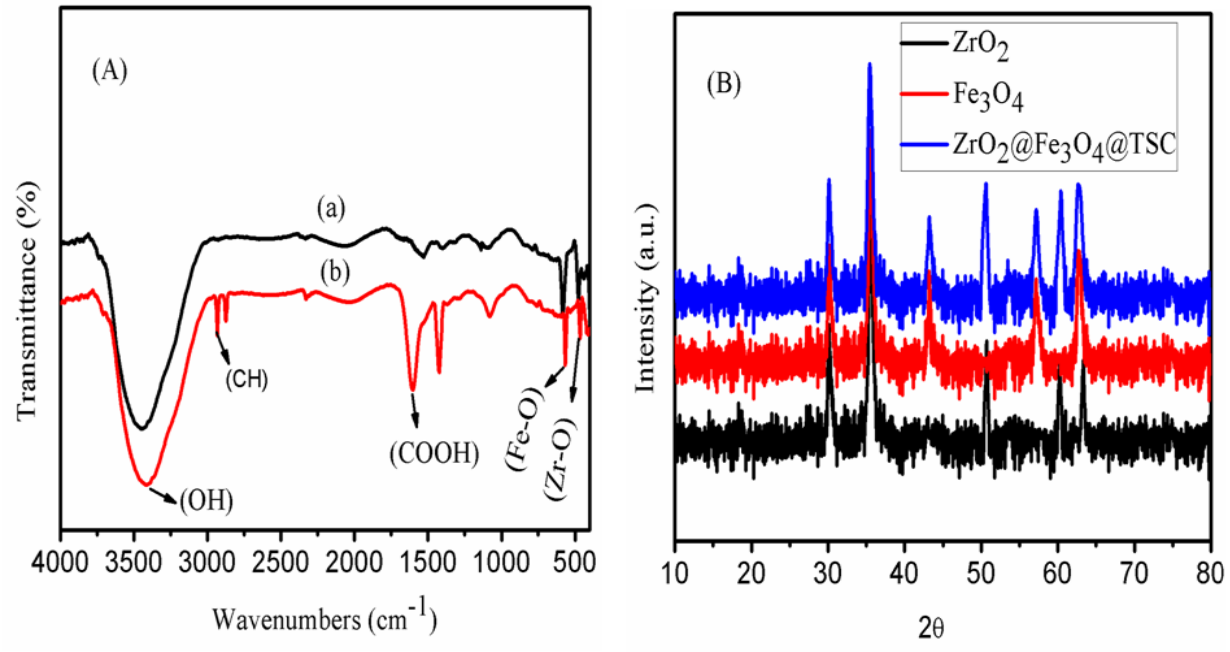

Fig. 1. (A) FT-IR spectrum of (a) ZrO_2@Fe_3O_4 MNPs and (b) ZrO_2@Fe_3O_4@TSC MNPs (B) the powder XRD pattern of the sample

Figure 1B shows the X-ray diffraction patterns of ZrO_2 nanoparticles, Fe_3O_4 nanoparticles, and ZrO_2@Fe_3O_4@TSC magnetic nanocomposites. The diffraction peaks observed at 2θ = 30.5°, 35.2°, 50.7°, 60.4°, and 63.3° can be indexed to the (111), (200), (220), (311), and (222) planes of cubic ZrO_2, in agreement with JCPDS card no. 27-0997. Similarly, the peaks at 30.08°, 35.3°, 43.6°, 57.1°, and 62.6° correspond to the (220), (311), (400), (333), and (440) planes of Fe_3O_4, confirming its spinel cubic structure in accordance with JCPDS card no. 82-1533. The broadening of the diffraction peaks in the ZrO_2@Fe_3O_4@TSC nanocomposite indicates nanoscale crystallite size and suggests enhanced surface interactions after TSC stabilization. These XRD results, together with the FTIR data, confirm the successful synthesis and stabilization of the magnetic ZrO_2@Fe_3O_4@TSC nanocomposite.

Table 1

Comparison of Adsorption Capacity of Various Sorbents with ZrO_2@Fe_3O_4@TSC Nanocomposites onto Cd (II) Ions

Reference	Adsorbent	q_{max} (mg/g)
Present study	ZrO_2@Fe_3O_4@TSC nanocomposites	50.26
[68]	Multiwalled carbon	10.86
[69]	$Cu_3(BTC)_2$-SH	74.50
[69]	$Cu_3(BTC)_2$	67.80
[70]	Si-DTC	43.47
[71]	PPBM	43.48
[72]	Fe_3O_4-GS	27.83
[73]	Fe_3O_4-cyclodextrin	22.70
[74]	Fe_3O_4-P(Cys/HEA) hydrogel	19.50
[75]	MDM	31.40

Journal of Chemistry and Technologies, 2026, *34*(1), 71-85

TEM analysis

Transmission electron microscopy was used to examine the size and morphology of ZrO_2@Fe_3O_4 and ZrO_2@Fe_3O_4@TSC magnetic nanoparticles. As shown in Figure 2A, the ZrO_2@Fe_3O_4 nanoparticles exhibited well-defined cubic and spherical morphologies. In Figure 2B, the ZrO_2@Fe_3O_4@TSC nanoparticles appear somewhat aggregated, which may be attributed to the presence of surface hydroxyl groups and magnetic interactions between particles. In addition, the energy-dispersive X-ray spectrum shown in Figure 2C confirms the presence of Fe, Zr, O, and C, thereby verifying the composition and successful synthesis of the nanocomposite.

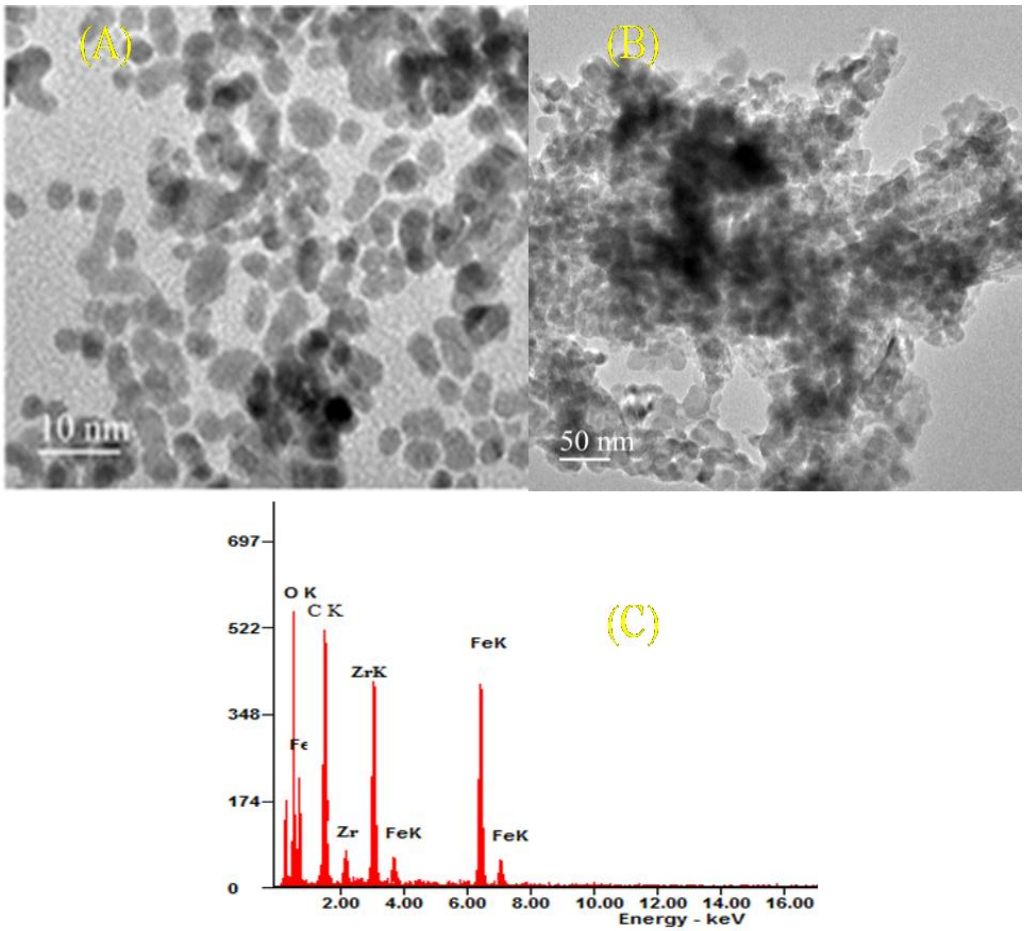

Fig. 2. (A)TEM images of the ZrO_2@Fe_3O_4 MNPs at 10 nm (B) TEM images of the ZrO_2@Fe_3O_4@TSC MNPs at 50 nm (C) EDX pattern of ZrO_2@Fe_3O_4@TSC MNPs

VSM study

The magnetization (M-H) curves of ZrO_2@Fe_3O_4 and ZrO_2@Fe_3O_4@TSC nanocomposites obtained by vibrating sample magnetometry are shown in Figure 3. The hysteresis loop of the ZrO_2@Fe_3O_4 nanoparticles confirms their ferromagnetic behavior, with a saturation magnetization value of approximately 10.9 emu g^{-1}. A similar magnetic response was observed for the ZrO_2@Fe_3O_4@TSC nanocomposite; however, its saturation magnetization decreased to 7.7 emu g^{-1} after TSC functionalization. This reduction in magnetization can be attributed to surface modification of the magnetic core by the organic ligand.

Journal of Chemistry and Technologies, 2026, *34*(1), 71-85

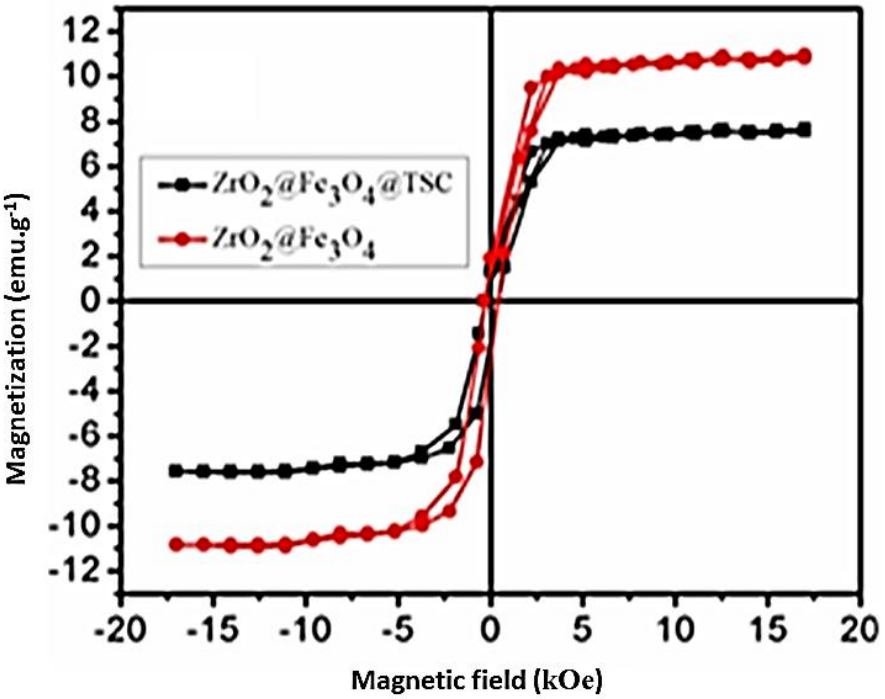

Fig. 3. (A) M-H hysteresis loop of ZrO_2@Fe_3O_4 MNPs and ZrO_2@Fe_3O_4@TSC MNPs sample measures at 300 K

pH effect on Cd (II) Adsorption

The effect of pH on Cd(II) adsorption is closely related to changes in metal-ion speciation, the surface charge of the adsorbent, and ion-exchange interactions. The synthesized ZrO_2@Fe_3O_4@TSC nanocomposite acted as an efficient adsorbent for the removal of Cd(II) ions from contaminated wastewater, and the solution pH played a crucial role in determining its adsorption performance. Experiments were carried out using Cd(II) solutions with pH values ranging from 2.0 to 8.0 and different initial metal concentrations. The results showed that the removal efficiency of Cd(II) increased gradually as the pH rose from 2.0 to 6.0, reaching its maximum at pH 6.0. At lower pH values, adsorption was suppressed because of the high concentration of H^+ ions competing with Cd(II) ions for active sites on the adsorbent surface. At pH values above 6.0, the adsorption efficiency decreased, likely because of the formation of cadmium hydroxyl species such as $Cd(OH)^+$ and $Cd(OH)_2$, which reduce the availability of free Cd(II) ions in solution. The maximum removal efficiency of 95.6 % was achieved at a Cd(II) concentration of 50 mg L^{-1} and pH 6.0, indicating that these were the optimum conditions for Cd(II) adsorption onto the ZrO_2@Fe_3O_4@TSC nanocomposite.

Table 2

Kinetic Parameters for the Adsorption of Cd (II) onto ZrO_2@Fe_3O_4@TSC Nanocomposites at Different Concentrations

ZrO_2@Fe_3O_4@TSC nanocomposites	Lagergren first order			Pseudo-second-order		
	K_1 (1/min)	R^2	SSE	K_2 (g/mg.min)	R^2	SSE
40	0.023	0.0985	0.983	0.014	0.999	0.912
50	0.028	0.979	0.987	0.018	0.999	0.915
60	0.034	0.976	0.980	0.022	0.998	0.916

Outcomes of contact time on Cd (II) adsorption kinetics study:

The impact of contact time on Cd (II) adsorption was observed at pH 6.0 by using the sample Cd (II) concentration of 50 mg L^{-1}. The adsorption method displayed rapid approval for kinetics experimental of Cd (II) sorption with whole sample, nevertheless, the kinetic study information not fixed and align with the pseudo-first-order model when applied to ZrO_2@Fe_3O_4@TSC nanocomposites [63]. The pseudo first order kinetic model is mathematically expressed as follows:

$$\log(qe - qt) = \log qe - \left(\frac{k1}{2.303}\right) t \qquad (3)$$

where k_1 (min^{-1}) is the pseudo first order rate constant of adsorption, qe and qt are the amount of the Cd (II) removal per unit mass of adsorbed (mg/g) at equilibrium and at time t (min). The pseudo first order kinetic constant (k_1) study was found out from the slope of the plot of log (qe-qt) vs. time (t). The R^2 value is clearly examined that

Journal of Chemistry and Technologies, 2026, *34*(1), 71-85

less revealing of that adsorption of Cd (II) ions does not follow pseudo first order kinetic model (Table 2). The pseudo first order kinetic model revealed that the comparatively low relationship for correlation coefficient (R^2) values throughout experimental data at different concentrations. This data is signifying that its insufficiency for accurately recitation in the adsorption behavior of Cd (II) onto ZrO_2@Fe_3O_4@TSC nanocomposites (Table 1). Subsequently, this model is not suitable for characterizing the adsorption process. The kinetic analysis suggests that, therefore, an alternative model such as the pseudo-second-order model may offer a more precise depiction of this adsorption study. In this context, *Nakhlestani N. et al*. was found that the adsorption kinetics study and highlighting the kinetic model for adsorption heavy metal on the surface of nanocomposite by adsorption process of heavy metals such as Cd (II) ions onto a modified graphene oxide nanocomposite by using pseudo-second-order model [64].

In the interim, the present kinetic statistics were further studied by using pseudo second order kinetic model. The linear form of pseudo second order kinetic model is elucidated by the equation:

$$\frac{t}{q_t} = \frac{1}{K_2 q_e^2} + \frac{t}{q_e} \qquad (4)$$

where K_2 (g/mg min) is the pseudo second order rate constant of adsorption, q_e and q_t are the amount of the Cd (II) removal per unit mass of adsorbent (mg/g) at equilibrium and at time (min). The values of K_2 and q_e can be calculated from the slope intercept of $\frac{t}{q_t}$ vs t graph and it cab illustrated in the Figure 4.

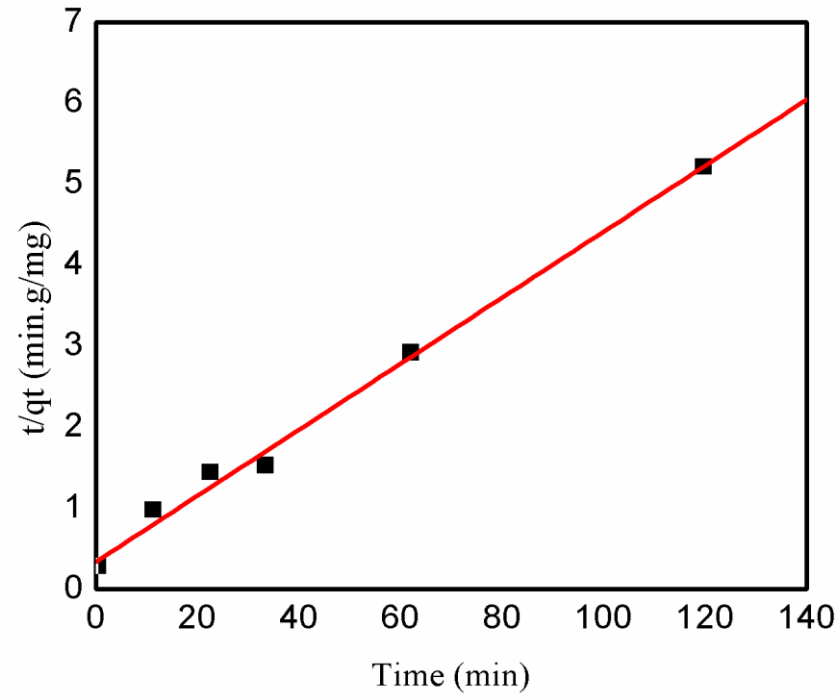

Fig. 4. Pseudo second order adsorption kinetics of Cd(II) on ZrO_2@Fe_3O_4@TSC MNPs sample

To assess the suitability of adsorption isotherm and kinetic models, experimental data were fitted using linear regression analysis. The goodness of fit was evaluated through statistical error functions, including the coefficient of determination (R^2), sum of squared errors (SSE), and chi-square test (χ^2). These parameters provide quantitative insight into the agreement between experimental and calculated adsorption values. The coefficient of determination (R^2) was employed to examine the linear correlation between experimental and predicted values, where values closer to unity indicate superior model applicability. R^2 was calculated using

$$R^2 = 1 - \frac{\sum\left(q_{e,exp} - q_{e,cal}\right)^2}{\sum\left(q_{e,exp} - \bar{q}_{e,exp}\right)^2} \qquad (5)$$

The sum of squared errors (SSE) was utilized to quantify the total deviation between experimentally observed adsorption capacities and model-predicted values:

$$SSE = \sum\left(q_{e,exp} - q_{e,cal}\right)^2 \qquad (6)$$

Journal of Chemistry and Technologies, 2026, *34*(1), 71-85

The chi-square statistical test (χ^2) was further applied to evaluate the consistency between experimental and calculated adsorption data:

$$\chi^2 = \sum \frac{(q_{e,exp} - q_{e,cal})^2}{q_{e,cal}} \qquad (7)$$

The adsorption isotherm constants derived from the experimental data are presented in Table 3. The Freundlich constant n was found to be less than 1, indicating favorable adsorption and a high affinity of the adsorbent for Cd(II) ions at low concentrations. Although the equilibrium data were fitted using both Langmuir and Freundlich isotherm models, the higher correlation obtained for the Langmuir model suggests that Cd(II) adsorption onto ZrO_2@Fe_3O_4@TSC nanocomposites predominantly occurs through monolayer coverage on a relatively uniform surface. This result also supports the assumption that chemisorption plays an important role in the adsorption process. Surface functionalization with the organic capping ligand appears to enhance both the adsorption capacity and the efficiency of Cd(II) removal by the magnetic nanoparticles. Comparison with previously reported adsorbents indicates that the prepared nanocomposite exhibits competitive adsorption performance for Cd(II) removal. Overall, the isotherm models provide valuable insight into the adsorption mechanism and the surface characteristics of the adsorbent. The adsorption data were well fitted by the pseudo-second-order kinetic model, with a correlation coefficient (R^2) of 0.999, indicating that this model accurately describes the adsorption process. In contrast, the pseudo-first-order model showed a lower correlation coefficient and was therefore less suitable for describing Cd(II) adsorption onto ZrO_2@Fe_3O_4@TSC nanocomposites. In the pseudo-second-order model, the plot of t/q_t versus t was used to determine the rate constant k_2 and the equilibrium adsorption capacity q_e, where t is the contact time and q_t is the amount of Cd(II) adsorbed per unit mass of adsorbent. These results confirm that the adsorption kinetics of Cd(II) on ZrO_2@Fe_3O_4@TSC nanocomposites follow the pseudo-second-order model.

Table 3

Langmuir and Freundlich Isotherm Constants and Correlation Coefficients for Cd (II) Adsorption onto ZrO_2@Fe_3O_4@TSC Nanocomposites at Constant Temperature

Temp. (K)	Langmuir				Freundlich			
	q_m (mg/g)	K_L (L/mg)	R^2	χ^2	K_f (mg/g)	1/n	R^2	χ^2
303	50.26	3.67	0.998	16.67	8.28	0.667	0.985	78.53

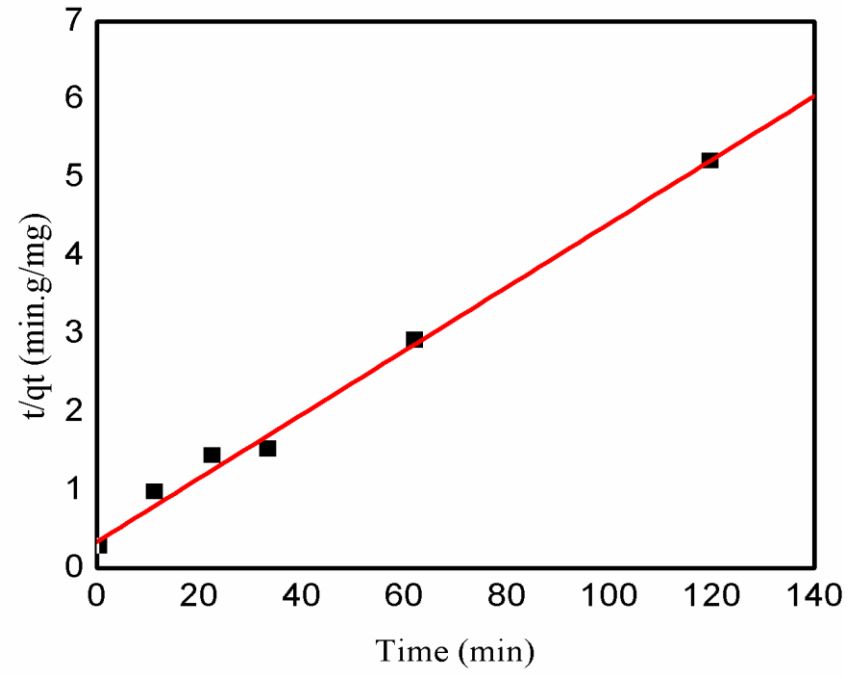

Journal of Chemistry and Technologies, 2026, *34*(1), 71-85

Fig. 4. Pseudo second order adsorption kinetics of Cd(II) on ZrO_2@Fe_3O_4@TSC MNPs sample

Adsorption isotherm analysis

Colloid chemistry clearly revealed about the adsorption phenomena due to their interpretation in various applications. Whereas the numerous chemical theories of adsorption have been projected, the predominant viewpoint of the amongst investigators is that adsorption is chiefly a physical process rather than a chemical one. The estimation of distribution Cd (II) ions, consequently, in the liquid/solid inter phase at equilibrium during adsorption, the room temperature adsorption capacities of Cd (II) were calculated at pH 6.0 using two typical adsorption models. The Langmuir isotherm explained monolayer adsorption on a solid surface, while the Freundlich isotherm explained multilayer adsorption with random distribution. The linearized form of the Langmuir isotherm [67] is represented as follows:

$$\frac{Ce}{qe} = \frac{Ce}{qm} + \frac{1}{qm\,b} \qquad (8)$$

where qe is the equilibrium metal ion concentration on the sorbent (mg/g), Ce is the equilibrium metal ion concentration in the solution (mg/L), qm is the maximum capacity of the adsorbent (mg/g) and b is the Langmuir constant related to the free energy of sorption. The values of qm (mg/g) and b were calculated from the slope and intercept of 1/Ce versus 1/qe (Figure 5). The maximum monolayer sorption capacity was found to be 50.26 mg/g of Cd (II) onto ZrO_2@Fe_3O_4@TSC nanocomposites. Additional parameter in the Langmuir isotherm a dimension less separation factor (RL) is defined as follows:

$$RL = \frac{1}{1 + bCi}, \qquad (9)$$

where Ci (mg/g) is the initial metal concentration, b is the Langmuir constant. For favorable adsorption, RL must lie within 0 to 1, where RL >1, RL = 1 and RL < 0 indicate the unfavorable linear and irreversible adsorption. In this study, the RL is 0.0918 which lies between 0 to 1. This indicates a highly favorable adsorption and increasing adsorption efficiency at higher Cd (II) concentrations.

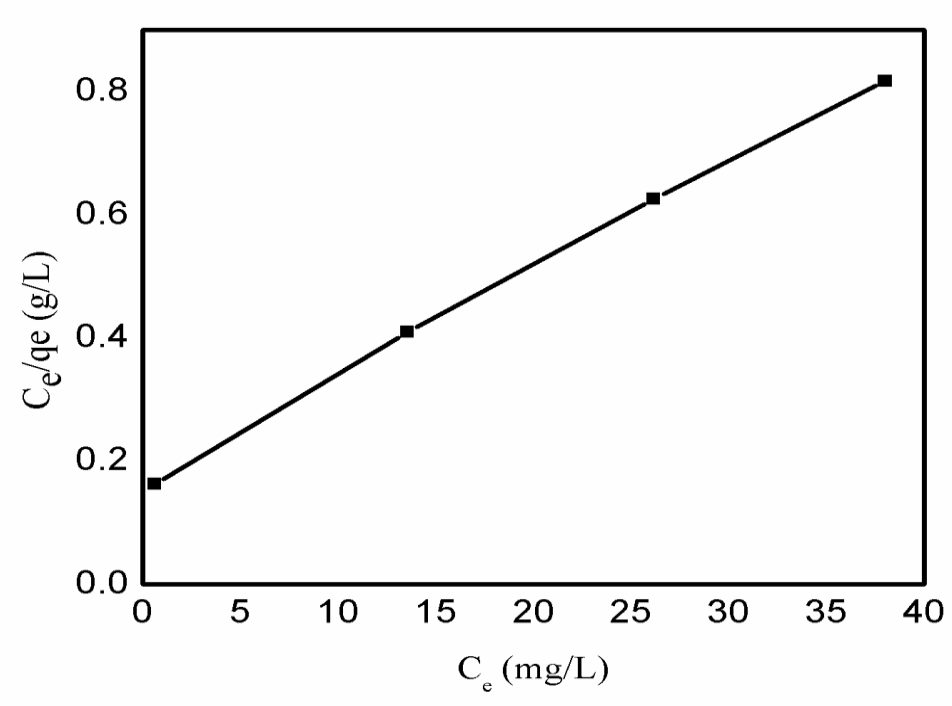

Fig. 5. Linear plot of Langmuir of Cd (II) on ZrO_2@Fe_3O_4@TSC MNPs sample

The Freundlich isotherm method can be normally used to define the adsorption of metal ions onto heterogeneous surfaces, and the linear form of isotherm is expressed as:

$$\log qe = \log kf + \frac{1}{n}\log Ce \qquad (10)$$

where k_f and n are the Freundlich isotherm constants that represent the adsorption of adsorbents. The linear Freundlich isotherm provided a good fit to the adsorption data (Figure. 6), providing a Cd (II) adsorption isotherm of ZrO_2@Fe_3O_4@TSC nanocomposites.

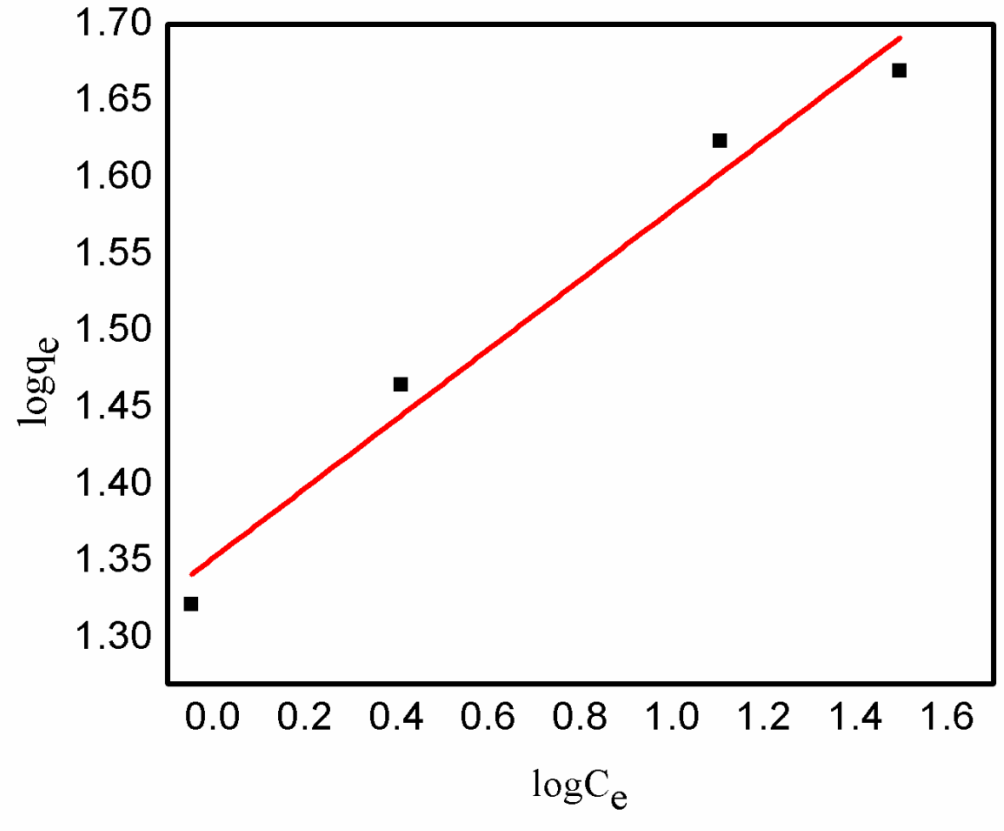

Fig. 6. Linear plot of Freundlich isotherm of Cd (II) on ZrO_2@Fe_3O_4@TSC MNPs sample

Conclusion

The synthesized ZrO_2@Fe_3O_4@TSC magnetic nanocomposite exhibited favorable structural, morphological, and magnetic properties for Cd(II) adsorption from aqueous solution. Characterization results showed that the material possessed a spherical morphology with particle sizes in the range of 16–20 nm. Magnetic measurements confirmed its ferromagnetic behavior, with a saturation magnetization of 7.7 emu/g, which makes the nanocomposite suitable for facile separation from aqueous media. Adsorption studies demonstrated that ZrO_2@Fe_3O_4@TSC is an effective adsorbent for Cd(II) removal. The kinetic data followed the pseudo-second-order model, indicating that chemisorption is the dominant adsorption mechanism. Equilibrium data were best fitted by the Langmuir isotherm model, suggesting monolayer adsorption on the surface of the nanocomposite. The maximum adsorption capacity was 50.26 mg/g at 303 K, confirming the potential of this nanocomposite as an efficient adsorbent for the removal of heavy metals from contaminated wastewater.

Acknowledgements

This work was supported by Gayatri Vidya Parishad College for Degree and PG Courses (A) Rushikonda, Visakhapatnam-530045, Andhra Pradesh, India.

References

[1] Abdelfattah, I., & El-Shamy, A. M. (2024). A comparative study for optimizing photocatalytic activity of TiO_2-based composites with ZrO_2, ZnO, Ta_2O_5, SnO, Fe_2O_3, and CuO additives. *Scientific Reports, 14*(1), 27175. https://doi.org/10.1038/s41598-024-77752-5

[2] Al-Mamun, M. R., Kader, S., Islam, M. S., & Khan, M. Z. H. (2019). Photocatalytic activity improvement and application of UV-TiO2 photocatalysis in textile wastewater treatment: A review. *Journal of Environmental Chemical Engineering, 7*(5), 103248. https://doi.org/10.1016/j.jece.2019.103248

[3] Yang, J., Hou, B., Wang, J., Tian, B., Bi, J., Wang, N., Li, X., & Huang, X. (2019). Nanomaterials for the removal of heavy metals from wastewater. *Nanomaterials, 9*(3), 424. https://doi.org/10.3390/nano9030424

[4] Putri, Y. E., Wendari, T. P., Dinda, D., Arnel, M., Faradilla, H., Refinel, R., & Efdi, M. (2024). The hydrothermal synthesis of SrTiO3 nanopolyhedral with the assistance of surfactants and their optical

characteristics. *Case Studies in Chemical and Environmental Engineering, 9*, 100601. https://doi.org/10.1016/j.cscee.2023.100601

[5] Mouden, A. E., Messaoudi, N. E., Guerraf, A. E., Bouich, A., Mehmeti, V., Lacherai, A., Jada, A., Americo-Pinheiro, J.H.P. (2023). Removal of cadmium and lead ions from aqueous solutions by noveldolomite-quartz@Fe_3O_4 nanocomposite fabricated as nanoadsorbent. *Environmental Research, 225*, 115606. https://doi.org/10.1016/j.envres.2023.115606

[6] Haounati, R., Ouachtak, H., Haouti, R. E., Akhouairi, S., Largo, F., Akbal, F., Benlhachemi, A., Jada, A., Addi, A. A. (2020). Elaboration and properties of a new SDS/CTAB@Montmorillonite organoclay composite as a superb adsorbent for the removal of malachite green from aqueous solutions. *Separation and Purification Technology, 255*, 117335. https://doi.org/10.1016/j.seppur.2020.117335

[7] Almeida, C. A. P., Debacher, N. A., Downs, A. J., Cottet, L., & Mello, C. A. D. (2009). Removal of methylene blue from colored effluents by adsorption on montmorillonite clay. *Journal of Colloid and Interface Science, 332*(1), 46–53. https://doi.org/10.1016/j.jcis.2008.12.012

[8] de Resende, V. G., Garcia, F. L., Peigney, A., De Grave, E., & Laurent, C. (2009). Synthesis of Fe-ZrO2 nanocomposite powders by reduction in H2 of a nanocrystalline $(Zr,Fe)O_2$ solid solution. *Journal of Alloys and Compounds, 471*(1-2), 204–210. https://doi.org/10.1016/j.jallcom.2008.03.045

[9] Wahba, M. A., Mohamed, W. A. A., & Hanna, A. A. (2016). Sol-gel synthesis, characterization of Fe/ZrO2 nanocomposites and their photodegradation activity on indigo carmine and methylene blue textile dyes. *International Journal of ChemTech Research, 9*(6), 914–925.

[10] Zeebaree, A. Y. S., Zeebaree, S. Y. S., Rashid, R. F., Zebari, O. I. H., Albarwry, A. J. S., Ali, A. F., Zebari, A. Y. S. (2022). Sustainable engineering of plant-synthesized TiO_2 nanocatalysts: Diagnosis, properties and their photocatalytic performance in removing of methyleneblue dye from effluent. *A review. Current Research in Green and Sustainable Chemistry, 5*, 100312. https://doi.org/10.1016/j.crgsc.2022.100312

[11] Daniel, S., Malathi, S., Balasubramanian, S., Sivakumar, M., & Sironmani, T. A. (2014). *Multifunctional silver, copper and zero valent iron metallic nanoparticles for wastewater treatment. In Application of Nanotechnology in Water*. John Wiley & Sons.

[12] Cheng, Q., Yang, W., Chen, Q., Zhu, J., Li, D., Fu, L., Zhou, L. (2020). Fe-doped zirconia nanoparticles with highly negative conduction band potential for enhancing visible light photocatalytic performance. *Applied Surface Science, 530*, 147291. https://doi.org/10.1016/j.apsusc.2020.147291

[13] Manyangadze, M., Chikuruwo, N. H. M., Narsaiah, T. B., Chakra, C. S., Radhakumari, M., & Danha, G. (2020). Enhancing adsorption capacity of nano-adsorbents via surface modification: A review. South African Journal of Chemical Engineering, 31, 25–32. https://doi.org/10.1016/j.sajce.2019.11.003

[14] Vo, L. Q., Anh-Tuan, V., Le, T. D., Huynh, C. D., Tran, H. V. (2024). Fe3O4/Graphene oxide/chitosan nanocomposite: A smart nanosorbent for lead (II) ion removal from contaminated water. *ACS Omega, 9*(15), 17506–17517. https://doi.org/10.1021/acsomega.4c00486

[15] Yasin, A. S., Mohamed, Y. A., Kim, D., Yoon, S., Ra, H., & Lee, K. (2021). Efficiency enhancement of electro-adsorption desalination using iron oxide nanoparticle-incorporated activated carbon nanocomposite. *Micromachines, 12*(10), 1148. https://doi.org/10.3390/mi12101148

[16] Hui, Y., & Zhang, S. (2021). A facile synthesis of Fe-doped zirconium oxide nanoparticles for enhancement of Rhodamine B dye degradation. *International Journal of Electrochemical Science, 16*(6), 210653. https://doi.org/10.20964/2021.06.53

[17] Sreelekha, N., Subramanyam, K., Reddy, D. A., Murali, G., Varma, K. R., & Vijayalakshmi, R. P. (2016). Efficient photocatalytic degradation of rhodamine-B by Fe doped CuS diluted magnetic semiconductor nanoparticles under the simulated sunlight irradiation. *Solid State Sciences, 62*, 71–81. https://doi.org/10.1016/j.solidstatesciences.2016.11.001

[18] Zhao, H., Song, F., Su, F., Shen, Y., & Li, P. (2020). Removal of cadmium from contaminated groundwater using a novel silicon/aluminum nanomaterial: An experimental study. *Archives of Environmental Contamination and Toxicology, 79*, 324–337. https://doi.org/10.1007/s00244-020-00784-1

[19] Liang, L., & Gong, P. (2020). Urban and air pollution: A multi-city study of long-term effects of urban landscape patterns on air quality trends. *Scientific Reports, 10*, 18618. https://doi.org/10.1038/s41598-020-74524-9

[20] Sarwar, N., Bibi, F. U. N., Junaid, A., & Alvi, S. (2024). Impact of urbanization and human development on ecological footprints in OECD and non-OECD countries. *Heliyon, 10*(18), e38058. https://doi.org/10.1016/j.heliyon.2024.e38058

[21] Siddiqua, A., Hahladakis, J. N., & Al-Attiya, W. A. K. A. (2022). An overview of the environmental pollution and health effects associated with waste landfilling and open dumping. *Environmental Science and Pollution Research, 29*, 58514–58536. https://doi.org/10.1007/s11356-022-21578-z

[22] Manisalidis, I., Stavropoulou, E., Stavropoulos, A., & Bezirtzoglou, E. (2020). Environmental and health impacts of air pollution: A review. *Frontiers in Public Health, 8*, 14. https://doi.org/10.3389/fpubh.2020.00014

[23] Münzel, T., Hahad, O., Daiber, A., & Landrigan, P. J. (2022). Soil and water pollution and human health: What should cardiologists worry about? *Cardiovascular Research, 118*(17), 3271–3273. https://doi.org/10.1093/cvr/cvac082

[24] Mustafa, B. M., & Hassan, N. E. (2024). Water contamination and its effects on human health: A review. *Journal of Geography, Environment and Earth Science International, 28*(1), 38–49. https://doi.org/10.9734/JGEESI/2024/v28i1743

[25] Khushbu, Gulati, R., Sushma, Kour, A., & Sharma, P. (2022). Ecological impact of heavy metals on aquatic environment with reference to fish and human health. *Journal of Applied and Natural Science, 14*(4), 1471–1484. https://doi.org/10.31018/jans.v14i4.3900

[26] Perera, P. A. C. T., Kodithuwakku, S. P., Sundarabarathy, T. V., & Edirisinghe, U. (2015). Bioaccumulation of cadmium in freshwater fish: An environmental perspective. *Insight Ecology, 4*(1), 1–12. https://doi.org/10.5567/ECOLOGY-IK.2015.1.12

[27] Naddafi, K., Nabizadeh, R., Saeedi, R., Mahvi, A. H., Vaezi, F., Yaghmaeian, K., Ghasri, A., & Nazmara, S. (2007). Biosorption of lead (II) and cadmium (II) by protonated Sargassum glaucescens biomass in a continuous packed bed column. *Journal of Hazardous Materials, 147*(3), 785–791. https://doi.org/10.1016/j.jhazmat.2007.01.082

[28] Sun, J., You-Peng, D., Xu, J., Feng-Min, Z., Qi-Yuan, H., Min-Min, T., Liu, Y., Yang, J., Hong-Yan, L., Fu, L., & Zhao, H. (2024). [Title of the specific article needed]. *Respiratory Research, 25*, 19. https://doi.org/10.1186/s12931-024-02726-0

[29] Ganguly, K., Levänen, B., Palmberg, L., Åkesson, A., & Lindén, A. (2018). Cadmium in tobacco smokers: A neglected link to lung disease? *European Respiratory Review, 27*(147), 170122. https://doi.org/10.1183/16000617.0122-2017

[30] Barregard, L., Bergström, G., & Fagerberg, B. (2014). Cadmium, type 2 diabetes, and kidney damage in a cohort of middle-aged women. *Environmental Research, 135*, 311–316. https://doi.org/10.1016/j.envres.2014.09.017

[31] Wu, M., Song, J., Zhu, C., Wang, Y., Yin, X., Huang, G., Zhao, K., Zhu, J., Duan, Z., & Su, L. (2017). Association between cadmium exposure and diabetes mellitus risk: A PRISMA-compliant systematic review and meta-analysis. *Oncotarget, 8*(68), 113129–113141. https://doi.org/10.18632/oncotarget.22820

[32] Bernard, A. (2004). Renal dysfunction induced by cadmium: Biomarkers of critical effects. *Biometals, 17*(5), 519–523. https://doi.org/10.1023/B:BIOM.0000045731.75602.b9

[33] Das, S., Sultana, K. W., Ndhlala, A. R., Mondal, M., & Chandra, I. (2023). Heavy metal pollution in the environment and its impact on health: Exploring green technology for remediation. *Environmental Health Insights, 17*, 11786302231201259. https://doi.org/10.1177/11786302231201259

[34] Lv, Y., Wang, P., Huang, R., Liang, X., Wang, P., Tan, J., Chen, Z., Dun, Z., Wang, J., Jiang, Q., Wu, S., Ling, H., Li, Z., & Yang, X. (2017). Cadmium exposure and osteoporosis: A population-based study and benchmark dose estimation in Southern China. *Journal of Bone and Mineral Research, 32*(10), 1990–2000. https://doi.org/10.1002/jbmr.3151

[35] Wang, M., Wang, X., Liu, J., Wang, Z., Jin, T., Zhu, G., & Chen, X. (2021). The association between cadmium exposure and osteoporosis: A longitudinal study and predictive model in a Chinese female population. *Frontiers in Public Health, 9*, 762475. https://doi.org/10.3389/fpubh.2021.762475

[36] Genchi, G., Sinicropi, M. S., Lauria, G., Carocci, A., & Catalano, A. (2020). The effects of cadmium toxicity. *International Journal of Environmental Research and Public Health, 17*(11), 3782. https://doi.org/10.3390/ijerph17113782

[37] Takeya, I., Etsuko, K., Yasushi, S., Mirei, U., Mitsuhiro, O., Hideaki, N., & Koji, N. (2005). Estimation of cumulative cadmium intake causing Itai-itai disease. *Toxicology Letters, 159*(2), 192–201. https://doi.org/10.1016/j.toxlet.2005.05.011

[38] Zarei, R., Sabokbar, A., Zarif, B. R., Bayat, M., & Haghnazari, N. (2024). Efficient biosorption of Zn (II), Cd (II), and Pb (II) by Aspergillus brasiliensis in industrial wastewater coupled with electrochemical monitoring via sensor enhanced with modified silver nanoparticles. *Environmental Science and Pollution Research.* https://doi.org/10.1007/s11356-024-35471-4

[39] Ahmad, I., Asad, R. U., Maryam, L., & Masood, M. (2024). *Treatment methods for cadmium removal from wastewater*. In Cadmium Toxicity in Water. Springer. https://doi.org/10.1007/978-3-031-54005-9_7

[40] Kim, J. J., Lee, S. S., Fenter, P., Myneni, S. C. B., Nikitin, V., & Peters, C. A. (2023). Carbonate coprecipitation for Cd and Zn treatment and evaluation of heavy metal stability under acidic conditions. *Environmental Science & Technology, 57*(8), 3104–3113. https://doi.org/10.1021/acs.est.2c07678

[41] Sunil, K., Karunakaran, G., Yadav, S., Padaki, M., Zadorozhnyy, V., & Pai, R. K. (2018). Al-Ti2O6 a mixed metal oxide based composite membrane: A unique membrane for removal of heavy metals. *Chemical Engineering Journal, 348*, 671–684. https://doi.org/10.1016/j.cej.2018.05.017

[42] Khan, Z., Elahi, A., Bukhari, D. A., & Rehman, A. (2022). Cadmium sources, toxicity, resistance and removal by microorganisms – A potential strategy for cadmium eradication. *Journal of Saudi Chemical Society, 26*(6), 101569. https://doi.org/10.1016/j.jscs.2022.101569

[43] Goswami, S., Aich, K., Das, S., Das, A. K., Manna, A., & Halder, S. (2013). A highly selective and sensitive probe for colorimetric and fluorogenic detection of Cd2+ in aqueous media. *Analytical Methods, 5*(11), 2658–2663. https://doi.org/10.1039/c3an36884j

[44] Peng, L., Chen, S., Song, H., Zheng, M., Luo, S., & Tie, B. (2023). Quick removal of suspended cadmium from irrigation water using water hyacinth (Eichhornia crassipes)-phosphoric fertilizer. *Water, Air, & Soil Pollution, 234*, 356. https://doi.org/10.1007/s11270-023-06365-x

[45] Vasudevan, S., & Lakshmi, J. (2011). Effects of alternating and direct current in electrocoagulation process on the removal of cadmium from water. *Journal of Hazardous Materials, 192*(1), 26–34. https://doi.org/10.1016/j.jhazmat.2011.04.081

[46] Santiago-Martínez, M. G., Lira-Silva, E., Encalada, R., Pineda, E., Gallardo-Pérez, J. C., Zepeda-Rodriguez, A., ... & Jasso-Chávez, R. (2015). Cadmium accumulation and toxicity in the microalga Euglena gracilis: Role of glutathione and phytochelatins. *Journal of Hazardous Materials, 288*, 104–112. https://doi.org/10.1016/j.jhazmat.2015.02.027

[47] Asad, R. U., Masood, M., Maryam, L., Waqas, H., Raza, E., & Ahmad, I. (2025). *Application of microbial technology for treatment of heavy metals contaminated wastewater.* In Smart *Waste and Wastewater Management by Biotechnological Approaches*. Springer. https://doi.org/10.1007/978-981-97-8673-2_17

[48] Bhagat, R., Walia, S. S., Kartik, S., Singh, R., Singh, G., & Hossain, A. (2024). The integrated farming system is an environmentally friendly and cost-effective approach to the sustainability of agri-food systems in the modern era of the changing climate: A comprehensive review. *Food and Energy Security, 13*(3), e534. https://doi.org/10.1002/fes3.534

[49] Kuppan, N., Padman, M., Mahadeva, M., Srinivasan, S., & Devarajan, R. S. (2024). A comprehensive review of sustainable bioremediation techniques: Eco-friendly solutions for waste and pollution management. *Waste Management Bulletin, 2*(3), 154–171. https://doi.org/10.1016/j.wmb.2024.07.005

[50] Bhattacharyya, K., Bhattacharjee, N., & Ganguly, S. (2023). Evidences for the augmented Cd (II) biosorption by Cd (II) resistant strain Candida tropicalis XTA1874 from contaminated aqueous medium. *Scientific Reports, 13*, 12034. https://doi.org/10.1038/s41598-023-38485-z

[51] Naseer, A. (2024). Role of nanocomposites and nano-adsorbents for heavy metals removal and dyes. An overview. *Desalination and Water Treatment, 320*, 100662. https://doi.org/10.1016/j.dwt.2024.100662

[52] Satyam, S., & Patra, S. (2024). Innovations and challenges in adsorption-based wastewater remediation: A comprehensive review. *Heliyon, 10*(5), e26573. https://doi.org/10.1016/j.heliyon.2024.e26573

[53] Akhtar, M. S., Ali, S., & Zaman, W. (2024). Innovative adsorbents for pollutant removal: Exploring the latest research and applications. *Molecules, 29*(18), 4317. https://doi.org/10.3390/molecules29184317

[54] Shahryari, T., Mostafavi, A., Afzali, D., & Rahmati, M. (2019). Enhancing cadmium removal by low-cost nanocomposite adsorbents from aqueous solutions; a continuous system. *Composites Part B: Engineering, 173*, 106963. https://doi.org/10.1016/j.compositesb.2019.106963

[55] Sangvanich, T., Morry, J., Fox, C., Ngamcherdtrakul, W., Goodyear, S., Castro, D., & Yantasee, W. (2014). Novel oral detoxification of mercury, cadmium, and lead with thiol-modified nanoporous silica. *ACS Applied Materials & Interfaces, 6*(8), 5483–5493. https://doi.org/10.1021/am5007707

[56] Alijani, H., Beyki, M. H., Fazli, Y., & Shariatinia, Z. (2017). A nanohybrid of mixed ferrite-polyaniline derivative copolymer for efficient adsorption of lead ions: Design of experiment for optimal condition, kinetic and isotherm study. *Desalination and Water Treatment, 66*, 338–345. https://doi.org/10.5004/dwt.2017.20196

[57] Panigrahy, S. K., Nandha, A., Chaturvedi, M., Mishra, P. K. (2024). Novel nanocomposites with advanced materials and their role in waste water treatment. *Next Sustainability, 4*, 100042. https://doi.org/10.1016/j.nxsust.2024.100042

[58] Nadaf, S., Jena, G. K., Rarokar, N., Gurav, N., Ayyanar, M., Prasad, S., & Gurav, S. (2023). Biogenic and biomimetic functionalized magnetic nanosystem: Synthesis, properties, and biomedical applications. *Hybrid Advances, 3*, 100038. https://doi.org/10.1016/j.hybadv.2023.100038

[59] Gerasimov, E. (2022). Synthesis of nanocomposites and catalysis applications. *Nanomaterials, 12*(5), 731. https://doi.org/10.3390/nano12050731

[60] Bhaskar, S., Awin, E. W., Kumar, K. C. H., Lale, A., Bernard, S., & Kumar, R. (2020). Design of nanoscaled heterojunctions in precursor derived t-ZrO2/SiOC(N) nanocomposites: Transgressing the boundaries of catalytic activity from UV to visible light. *Scientific Reports, 10*, 740. https://doi.org/10.1038/s41598-019-57394-8

[61] Safari, J., Gandomi-Ravandi, S., & Haghighi, Z. (2016). Supported polymer magnets with high catalytic performance in the green reduction of nitroaromatic compounds. *RSC Advances, 6*(38), 31514–31525. https://doi.org/10.1039/c5ra26613k

[62] Boamah, P. O., Huang, Y., Hua, M., Zhang, Q., Liu, Y., Onumah, J., Wang, W., & Song, Y. (2015). Removal of cadmium from aqueous solution using low molecular weight chitosan derivative. *Carbohydrate Polymers, 122*, 255–264. https://doi.org/10.1016/j.carbpol.2015.01.004

[63] Kowanga, K. D., Gatebe, E., Mauti, G. O., & Mauti, E. M. (2016). Kinetic, sorption isotherms, pseudo-first-order model and pseudo-second-order model studies of Cu(II) and Pb(II) using defatted Moringa oleifera seed powder. *The Journal of Phytopharmacology, 5*(2), 71–78.

[64] Nakhlestani, N., Taghavi, L., Dehghani, M., & Panahi, H. A. (2024). Efficient removal of Pb (II) and Cd (II) ions from aqueous solutions using a 5-aminoisophthalic acid polymerized magnetic graphene oxide composite. *Iranian Journal of Chemistry and Chemical Engineering, 43*(7), 2721–2736.

[65] Raven, K. P., Jain, A., & Loeppert, R. H. (1998). Arsenite and arsenate adsorption on ferrihydrite: Kinetics, equilibrium and adsorption envelopes. *Environmental Science & Technology, 32*(3), 344–349. https://doi.org/10.1021/es970421p

[66] Dada, A. O., Adekola, F. A., Odebunmi, E.O., Ogunlaja, A.S., & Bello, O. S. (2021). Two-three parameters isotherm

modeling, kinetics with statistical validity, desorption and thermodynamic studies of adsorption of Cu(II) ions onto zerovalent iron nanoparticles. *Scientific Reports, 11*, 16454. https://doi.org/10.1038/s41598-021-95090-8

[67] Langmuir, I. (1918). The adsorption of gases on plane surfaces of glass, mica and platinum. *Journal of the American Chemical Society, 40*(9), 1361–1403. https://doi.org/10.1021/ja02242a004

[68] Li, Y. H., Ding, J., Luan, Z., Di, Z., Zhu, Y., Xu, C., Wu, D., & Wei, B. (2003). Competitive adsorption of Pb2+, Cu2+ and Cd^{2+} ions from aqueous solutions by multiwalled carbon nanotubes. *Carbon, 41*(14), 2787–2792. https://doi.org/10.1016/S0008-6223(03)00392-0

[69] Wang, Y., Ye, G., Chen, H., Hu, X., Niu, Z., & Ma, S. (2015). Functionalized metal-organic framework as a new platform for efficient and selective removal of cadmium (II) from aqueous solution. *Journal of Materials Chemistry A, 3*(29), 15292–15298. https://doi.org/10.1039/c5ta03201f

[70] Bai, L., Hu, H. P., Fu, W., Wan, J., Cheng, X., Zhuge, L., Xiong, L., & Chen, Q. (2011). Synthesis of a novel silica-supported dithiocarbamate adsorbent and its properties for the removal of heavy metal ions. *Journal of Hazardous Materials, 195*, 261–275. https://doi.org/10.1016/j.jhazmat.2011.08.038

[71] Dubey, A., Mishra, A., & Singhal, S. (2014). Application of dried plant biomass as novel low-cost adsorbent for removal of cadmium from aqueous solution. *International Journal of Environmental Science and Technology, 11*, 1043–1050. https://doi.org/10.1007/s13762-013-0278-0

[72] Guo, X., Du, B., Wei, Q., Yang, J., Hu, L., Yan, L., & Xu, W. (2014). Synthesis of amino functionalized magnetic graphenes composite material and its application to remove Cr(VI), Pb(II), Hg(II), Cd(II) and Ni(II) from contaminated water. *Journal of Hazardous Materials, 278*, 211–220. https://doi.org/10.1016/j.jhazmat.2014.05.075

[73] Badruddoza, A. Z. M., Shawon, Z. B. Z., Daniel, T. W. J., Hidajat, K., & Uddin, M. S. (2013). Fe3O4/cyclodextrin polymer nanocomposites for selective heavy metals removal from industrial wastewater. *Carbohydrate Polymers, 91*(1), 322–332. https://doi.org/10.1016/j.carbpol.2012.08.030

[74] Hua, R., & Li, Z. (2014). Sulfhydryl functionalized hydrogel with magnetism: Synthesis, characterization and adsorption behavior study for heavy metal removal. *Chemical Engineering Journal, 249*, 189–200. https://doi.org/10.1016/j.cej.2014.03.097

[75] Lemessa, G., Chebude, Y., Demesa, A. G., Fadeev, E., Koiranen, T., & Alemayehu, E. (2024). Development of suitable magnetite–diatomite nanocomposite for Cd (II) adsorptive removal from wastewater. *Scientific African, 24*, e02213. https://doi.org/10.1016/j.sciaf.2024.e02213